Analysis and Design of Weakly Coupled LC Oscillator Arrays Based on Phase-Domain Macromodels

Paolo Maffezzoni, *Member, IEEE*, Bichoy Bahr, *Student Member, IEEE*, Zheng Zhang, *Student Member, IEEE*, and Luca Daniel, *Member, IEEE*

***Abstract*—An array of weakly coupled oscillators can generate multiphase signals, i.e., multiple sinusoidal signals with specific phase separations. Multiphase oscillators are attractive solutions in many electronic applications such as the synchronization of multiple processing units in digital electronics and the frequency synthesis in mixed-signal radio frequency circuits. Due to the complexity of multiphase oscillators and the large number of design parameters, novel simulation techniques are highly desired to efficiently handle such large-scale problems. In this paper, an efficient phase-domain simulation technique is proposed to calculate the phase response of inductance capacitance oscillator array. By some practical examples, it is shown how the proposed method can be exploited to identify the array topologies and parameter settings that guarantee stable phase separations. It is also shown how the proposed technique can be used to evaluate phase-noise performance.**

***Index Terms*—Coupled oscillators, phase-domain modeling, stochastic simulation.**

I. Introduction

THE TERM multiphase oscillator refers to an array of coupled oscillators that can generate iso-frequency sinusoidal signals with prescribed phase separations. These devices have many applications in radio frequency synthesizers and multiphase sampling clocks [1], [2]. For these applications, precise output phase differences and low phase-noise degradation are key figures of merit. In addition, new emerging technologies will soon allow efficient, large-scale integration of oscillator arrays. One example of such technologies is the CMOS-integrated microelectromechanical systems (MEMS) device resonant body transistor, which has demonstrated quality factors comparable to inductance capacitance (LC) tanks ($Q \sim 25$) while occupying orders of magnitude smaller area (device footprint $< 15\,\mu m^2$) [3]. In practical implementations, weak coupling is particularly appealing since it can be realized with auxiliary devices at the cost of negligible power dissipation. In addition, resonant or LC oscillators are preferred to other topologies (e.g., ring oscillators) since they are able to generate almost sinusoidal signals, with high harmonic purity, while ensuring a good phase noise/power tradeoff [4].

Designing an array composed of many oscillators with well precise phase separation is a challenging task. Even if one considers the array topology with almost identical oscillators and with couplings only limited to nearest-neighbor, referred to as chain array, the number of design parameters and degrees of freedom remain very large. In fact, the chain array may be open at the end or closed with a feedback path; the coupling between two oscillators may be unidirectional or bidirectional; the direction and strength of couplings may change along the chain [4]–[6]. While some studies have been presented for particular settings of parameters, a more general analysis and design methodology is still lacking. In this paper, we propose a solution by adopting a phase-domain macromodel for the multiphase oscillator. Our analysis aims at finding some simple rules for the design of multiphase LC oscillators organized in a chain. Macromodeling techniques have already been used in the literature to study frequency locking/pulling in a single oscillator or in two mutually coupled oscillators [7]–[9].

A. Our Contribution

The novel contributions of this paper are summarized as follows.

1) The phase-domain macromodeling technique is extended to an array of many coupled oscillators and it is utilized to determine the stable phase differences.
2) For the practically-relevant case of LC oscillators arranged in a chain array, topologies and coupling parameters are identified, which allows designers to obtain well precise phase separations.
3) The output phase noise of the multiphase oscillator is determined via some original closed-form expressions. The dependence of the output phase noise on the array topology and coupling parameters is studied in detail.

B. Paper Organization

Section II reviews briefly the phase-domain modeling and phase noise in a single oscillator. In Section III, we describe the nonlinear phase-domain model for a generic multiphase

Manuscript received April 24, 2014; revised July 28, 2014; accepted October 10, 2014. Date of publication October 27, 2014; date of current version December 17, 2014. This work was supported by the Progetto Roberto Rocca MIT-PoliMI and by the NSF-NEEDs program. This paper was recommended by Associate Editor V. Narayanan.

P. Maffezzoni is with the Politecnico di Milano, Milan 20133, Italy (e-mail: pmaffezz@elet.polimi.it).

B. Bahr, Z. Zhang, and L. Daniel are with the Massachusetts Institute of Technology, Cambridge, MA 02139 USA (e-mail: bichoy@mit.edu; z_zhang@mit.edu; luca@mit.edu).

Color versions of one or more of the figures in this paper are available online at http://ieeexplore.ieee.org.

Digital Object Identifier 10.1109/TCAD.2014.2365360

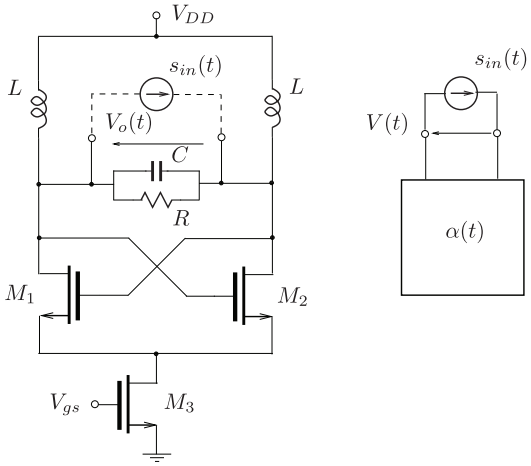

Fig. 1. LC oscillator. Left: circuit. Right: the phase-domain model.

oscillator and the related stochastic equation in the presence of noise. In Section IV, we focus on LC oscillators arranged in a chain array. Section V demonstrates the results of numerical experiments and derives some design rules.

II. Modeling Single Oscillator

Let us consider an electrical oscillator in free running, the output steady-state response of which is given as

$$V_0(t) = p(\omega_0 t) \tag{1}$$

where $\omega_0 = 2\pi f_0$ is the oscillating angular frequency, $T_0 = 1/f_0$ the period, and $p(\cdot)$ denotes a generic 2π-periodic function of its argument. Phase-domain macromodels are well suited to describe the oscillator response in the presence of deterministic weak perturbations or stochastic noise as its briefly reviewed below.

A. Phase-Domain Response to Weak Perturbation

In the presence of a small-amplitude injected signal $s_{\text{in}}(t)$, the response of the perturbed oscillator is well approximated by the phase model

$$V(t) = V_0(t + \alpha(t)) = p\left(\omega_0(t + \alpha(t))\right) \tag{2}$$

where the $\alpha(t)$ function represents the time-dependent time-shift of perturbed response with respect to the free-running one.

The product $\phi(t) = \omega_0\alpha(t)$ gives the related excess phase variable. It has been proved that $\alpha(t)$ depends on the injected signal through the following nonlinear differential equation:

$$\dot{\alpha}(t) = \Gamma(t + \alpha(t))s_{\text{in}}(t) \tag{3}$$

where $\Gamma(t)$ is a T_0-periodic function that describes the phase sensitivity to the particular injecting source [10], [11]. For LC oscillators the output response and phase model parameters assume particular values. As an example, Fig. 1 shows the LC oscillator topology that will be considered in this paper. With the parameters in Table I, the circuit oscillates at the frequency of 1.0261 GHz and its output voltage $V_0(t)$ measured across the LC tank is shown in Fig. 2. In the same figure, the $\Gamma(t)$ function (scaled by the factor 50) related to

TABLE I
Parameters of the LC Oscillator

Parameter	Value
V_{DD}	2.5 V
V_{gs}	1.0 V
C	0.3 pF
L	40 nH
R	11 kΩ
$(W/L)_{1,2}$	10
$(W/L)_3$	33

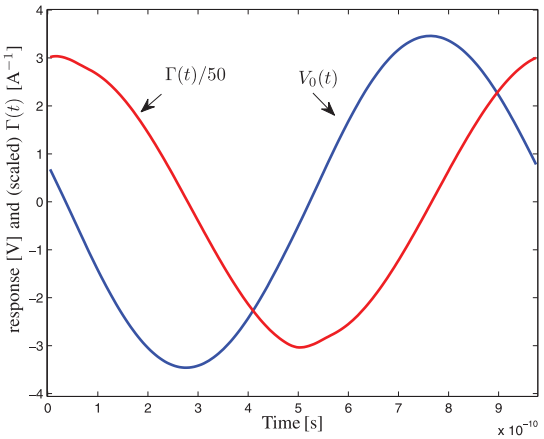

Fig. 2. Free-running response and function $\Gamma(t)$ of an LC oscillator.

a current perturbation $s_{\text{in}}(t)$ injected at the output terminals is also plotted. This figure highlights the following properties that hold for LC-based oscillators: 1) the output response is almost sinusoidal and 2) the related $\Gamma(t)$ is almost sinusoidal as well and is delayed by a $\pi/2$ phase angle. This can be formalized mathematically as

$$\begin{aligned} V_0(t) &= V_M \cos(\omega_0 t + \pi/2) \\ \Gamma(t) &= \Gamma_M \cos(\omega_0 t) \end{aligned} \tag{4}$$

where V_M and Γ_M are the peak values of the two sinusoids.

B. Modeling Phase Noise

Noise sources internal to the oscillator circuit introduce stochastic fluctuations to the time-shift variable $\alpha(t)$ and to the associated phase noise. This can be described, in a compact way, by the following average stochastic equation [12]–[14]:

$$\dot{\alpha}(t) = n_{\text{eq}}(t) = n^W_{\text{eq}}(t) + n^F_{\text{eq}}(t) \tag{5}$$

in which $n^W_{\text{eq}}(t)$ and $n^F_{\text{eq}}(t)$ are the macro noise sources that reproduce the global effect of all white and flicker noise sources in the oscillator circuit, respectively. Thus, $n^W_{\text{eq}}(t)$ is a zero-mean Gaussian process of constant power spectral density (PSD) $S^W_{\text{eq}}(f) = S^W_{\text{eq}}$, while $n^F_{\text{eq}}(t)$ is a process with PSD $S^F_{\text{eq}}(f) = S^F_{\text{eq}}/f$. In the frequency domain, we can derive the PSD of the phase noise variable $\phi(t) = \omega_0\alpha(t)$ as follows:

$$S_\phi(f) = \frac{f_0^2}{f^2} \times \left(S^W_{\text{eq}} + S^F_{\text{eq}}/f\right). \tag{6}$$

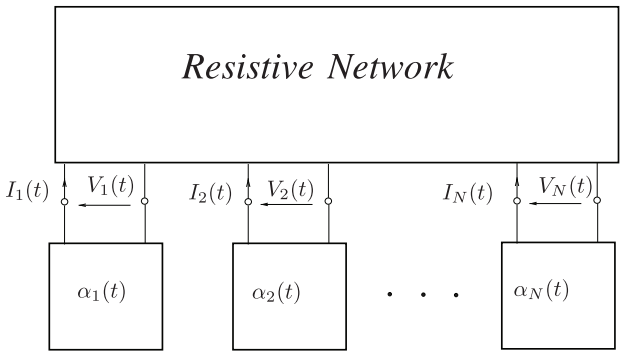

Fig. 3. Array of N weakly coupled oscillators.

The macromodel parameters S_{eq}^{W} and S_{eq}^{F} can be extracted via phase-noise measurements or detailed transistor-level phase-noise simulations [16].

III. Array of Resistively Coupled Oscillators

In this section, we provide the phase-domain macromodel for an array of N oscillators which are weakly coupled through a resistive N-port network described by its conductance matrix $G = \{g_{jk}\} \in \mathbb{R}^{N\times N}$, as shown in Fig. 3. In integrated CMOS circuits, coupling between oscillators is commonly realized through differential-pair transistors [4], [15] that can be realistically modeled as resistive transconductance elements, as described in the next section.[1]

A. Phase Response

We focus first on the phase response of the array. To this aim, we denote with $V_k(t)$ and ω_k the output response and angular frequency, respectively, of the kth oscillator when working in free-running mode and with $\Gamma_k(t)$ the associated phase-sensitivity function. Similarly, we denote with $\alpha_k(t)$ and $\phi_k(t) = \omega_k \alpha_k(t)$ the time-shift and excess phase of the kth oscillator which arise when the oscillator is connected to the coupling network and thus it is injected by a current $I_k(t)$.

By extending the method described in the previous section, we find

$$\begin{aligned} \dot{\alpha}_k(t) &= \Gamma_k(t+\alpha_k(t))I_k(t) \\ I_k(t) &= \sum_{j=1}^{N} g_{kj}\, V_j(t+\alpha_j(t)) \end{aligned} \tag{7}$$

which results in the following set of ordinary differential equations (ODEs):

$$\dot{\alpha}_k(t) = \Gamma_k(t+\alpha_k(t)) \times \sum_{j=1}^{N} g_{kj}\, V_j(t+\alpha_j(t)) \tag{8}$$

with $k = 1, \ldots, N$.

The mutual synchronization regime is achieved when, asymptotically for $t \to \infty$, the phase difference between any couple of oscillators remains bounded [17], i.e., when the following condition:

$$|\omega_k t + \phi_k(t) - \omega_j t - \phi_j(t)| < \epsilon' \tag{9}$$

[1]For the small-area transistors used to realize weak coupling, parasitic capacitances are in fact negligible.

holds for any k and j, where ϵ' is a constant value. A scenario of particular interest in practical applications is an array formed of N identical oscillators and thus with the same frequency $\omega_k = \omega_0$ for any k. In practical circuit implementations, mismatches among oscillators may introduce small differences (i.e., detunings) in the free-running oscillating frequencies ω_k. However, as long as detunings are small compared to the locking range [9], [17] they vanish at synchronization and thus can be neglected.

Under this condition, the synchronization condition can be rewritten as follows:

$$|\alpha_k(t) - \alpha_j(t)| < \epsilon. \tag{10}$$

At synchronization, the variables $\alpha_k(t)$ need not to be bounded and in fact they may grow almost linearly with time [17]. In general, we can thus assume that asymptotically, for $t \to \infty$, variables $\alpha_k(t)$ approach the waveforms $\widetilde{\alpha}_k(t)$ of the type

$$\widetilde{\alpha}_k(t) = \bar{\alpha}_k + m\, t + o_k(t) \tag{11}$$

where $\bar{\alpha}_k$ is a constant term varying along the array, m is a constant slope value, identical for all oscillators, and $o_k(t)$ is a small-amplitude high-frequency oscillating term with zero mean value.

Neglecting the rapidly oscillating terms $o_k(t)$, on average, the excess phase of oscillators tend asymptotically to the waveforms

$$\phi_k(t) = \omega_0 \bar{\alpha}_k + \omega_0 m\, t \tag{12}$$

and the phase difference between any two oscillators approaches a constant value given by

$$\phi_k(t) - \phi_j(t) = \bar{\phi}_k - \bar{\phi}_j = \omega_0 \left(\bar{\alpha}_k - \bar{\alpha}_j\right). \tag{13}$$

The challenge in applications is just to design an oscillator array such that well precise and stable phase separations (13) can be achieved. It is also worth noting that the presence of the term $m\,t$ in (11) implies that the common oscillating frequency ω_c of the array differs from the free-running one ω_0. In fact, replacing (11) in (2) and neglecting $o_k(t)$, we obtain

$$p\left((\omega_0 + \omega_0\, m)\, t + \bar{\alpha}_k\right) \tag{14}$$

which gives

$$\omega_c = \omega_0(1+m). \tag{15}$$

For weak coupling, we will find that $|m| << 1$ and thus the frequency correction (15) is very small.

B. Phase Noise

The noise sources internal to the kth oscillator in the array are represented by a macro noise source $n_{\text{eq}}^{k}(t)$ as explained in Section II-B. These internal noise sources produce extra random fluctuations $\tau_k(t)$, i.e., jitter, of the time shift $\alpha_k(t)$ variables around the regime waveforms $\widetilde{\alpha}_k(t)$, that is

$$\alpha_k(t) = \widetilde{\alpha}_k(t) + \tau_k(t). \tag{16}$$

The equations of the noisy array are given by the following set of stochastic differential equations:

$$\dot{\alpha}_k(t) = \Gamma_k(t+\alpha_k(t)) \times \sum_{j=1}^{N} g_{kj}\, V_j\left(t+\alpha_j(t)\right) + n_{\text{eq}}^k(t). \quad (17)$$

The stochastic equations above can be solved numerically by integration in time. In addition, since internal noise sources are small-amplitude signals, the random fluctuations $\tau_k(t)$ are small as well and thus (17) can be further expanded by linearization. To this aim, we plug (16) into (17) and adopt truncated Taylor expansions

$$\begin{aligned}\Gamma_k\left(t+\widetilde{\alpha}_k(t)+\tau_k(t)\right) &\approx \Gamma_k\left(t+\widetilde{\alpha}_k(t)\right) + \dot{\Gamma}\left(t+\widetilde{\alpha}_k(t)\tau_k(t)\right)\\ V_k\left(t+\widetilde{\alpha}_k(t)+\tau_k(t)\right) &\approx V_k\left(t+\widetilde{\alpha}_k(t)\right) + \dot{V}_k\left(t+\widetilde{\alpha}_k(t)\tau_k(t)\right).\end{aligned} \quad (18)$$

Neglecting the resulting second-order product terms $\tau_k(t)\tau_j(t)$ and higher order terms in (17) and using the fact that $\widetilde{\alpha}_k(t)$ solves (8) leads us to the linearized equations

$$\begin{aligned}\dot{\tau}_k(t) = &\left(\dot{\Gamma}_k\left(t+\widetilde{\alpha}_k(t)\right) \times \sum_{j=1}^{N} g_{kj}\, V_j\left(t+\widetilde{\alpha}_j(t)\right)\right)\tau_k(t)\\ &+ \Gamma_k\left(t+\alpha_k(t)\right) \times \sum_{j=1}^{N} g_{kj}\, \dot{V}_j\left(t+\widetilde{\alpha}_j(t)\right)\tau_j(t) + n_{\text{eq}}^k(t).\end{aligned} \quad (19)$$

The linearized equations above will be exploited in the next section to derive closed-form expressions for the phase noise in a chain array.

IV. Chain Array of LC Oscillators

The deterministic nonlinear ODE (8) and the related stochastic ODE (17) hold for generic oscillatory devices and for generic resistive coupling networks. In particular, they hold for nonharmonic oscillators (e.g., ring or relaxation oscillators) whose responses $V_k(t)$ and sensitivity functions $\Gamma_k(t)$ may contain many harmonic components. In this section, we consider more specific cases that are of great relevance in applications and for which we derive some practical design rules.

To this aim, we first suppose that the array is formed of N identical LC oscillators whose output response and phase sensitivity waveforms take the form reported in (4), for any k. The phase-domain response equations (8) become

$$\begin{aligned}\dot{\alpha}_k(t) = &\,\Gamma_M \cos(\omega_0 t + \omega_0\alpha_k(t))\\ &\times \sum_{j=1}^{N} g_{kj}\, V_M \cos\left(\omega_0 t + \omega_0\alpha_j(t) + \pi/2\right).\end{aligned} \quad (20)$$

Second, we focus on the relevant topology of the chain array where coupling arises only between nearest-neighbor oscillators. In integrated CMOS circuits, coupling between nearest oscillators is commonly realized through differential-pair transistors [15], as shown in Fig. 4. The differential current of coupling stages can be modeled by voltage-controlled current sources of transconductance $g = g_{k,j}$, as shown in Fig. 5(a) [4]. The magnitude of the transconductance $g_{k,j}$ gives the coupling

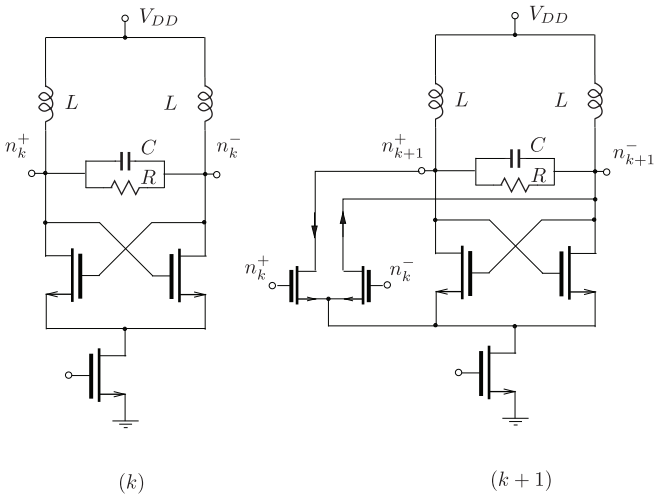

Fig. 4. Possible implementation of the coupling in a chain array by means of a differential stage.

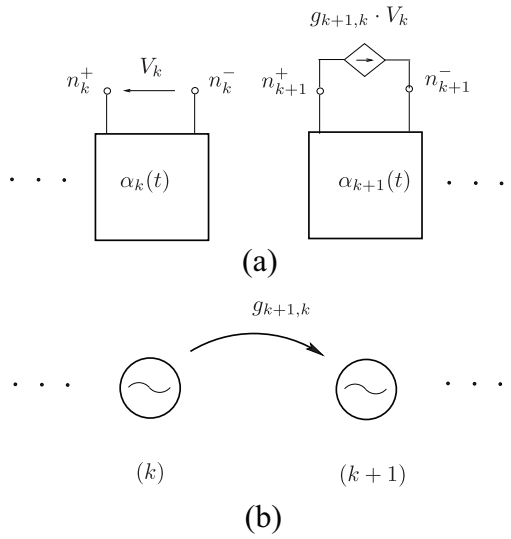

Fig. 5. Coupling in a chain array. (a) Voltage across the kth oscillator controls the current injected into the $k+1$ oscillator. (b) Schematic representation of this local coupling.

strength while its sign refers to the way the voltage-controlled current (i.e., the coupling differential stage) is connected to the terminals of the injected oscillator. To realize weak coupling among oscillators, injected currents should be kept one order of magnitude smaller than inner oscillator currents (i.e., inner transistor currents). Coupling is schematically represented with an oriented arch that points from the controlling device to the controlled/injected one, Fig. 5(b).

In practice, the chain array may have several possible topologies: coupling may be unidirectional (i.e., oscillator k injects into oscillator $k+1$) or bidirectional (i.e., oscillator k injects into oscillator $k+1$ and oscillator $k+1$ injects backward into oscillator k), the chain may be open at the two ends or may be closed with a feedback. Fig. 6 shows some of the possible topologies.

In the case of chain arrays, some theoretical results exist that prove the uniqueness of the achievable phase separation [6], [17]. To link our phase-domain model to these

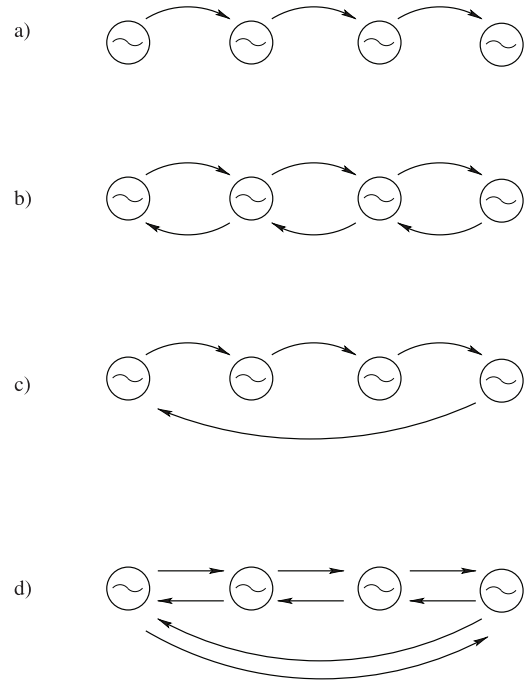

Fig. 6. Chain array topologies. (a) and (b) Open array with unidirectional and bidirectional coupling, respectively. (c) and (d) Unidirectional and bidirectional array closed in feedback.

theoretical results, we further develop equations (20) and use averaging [13], [14]. Keeping only the slowly varying terms resulting from the cosines product in (20) leads us to the following averaged equations for the excess phases $\phi_k(t) = \omega_0 \alpha_k(t)$:

$$\dot{\phi}_k(t) = B \sum_{j=1}^{N} g_{k,j} \sin\big(\phi_k(t) - \phi_j(t)\big) \tag{21}$$

with $g_{k,j} \neq 0$ only for $j = k-1$ and $j = k+1$ and

$$B = \frac{1}{2}\omega_0 \Gamma_M V_M. \tag{22}$$

Then, we make the difference between each equation in (21) for $\dot{\phi}_k(t)$ and the subsequent one for $\dot{\phi}_{k+1}(t)$, obtaining the following set of $(N-1)$ nonlinear coupled equations:

$$\begin{aligned}\dot{\psi}_k(t) = &-Bg_{k,k-1}\sin(\psi_{k-1}(t)) + Bg_{k,k+1}\sin(\psi_k(t)) \\ &+ Bg_{k+1,k}\sin(\psi_k(t)) - Bg_{k+1,k+2}\sin(\psi_{k+1}(t))\end{aligned} \tag{23}$$

with $k = 1, \ldots, N-1$, for the phase difference variables

$$\psi_k(t) = \phi_{k+1}(t) - \phi_k(t). \tag{24}$$

For a set of nonlinear equations having the structure of (23), it has been proved in [6] that there exist 2^{N-1} stationary solutions, i.e., with $\dot{\psi}_k(t) = 0$ but that only one of them is stable and thus observable in practice. This guarantees that in the case of a chain of LC oscillators, the numerical integration of the phase model (8) [or of its simplified version (20)] will supply the only phase separation set values (13) which is stable for a given chain topology. Therefore, the same phase separation will be obtained independently of the assumed initial phase condition.

We end this section by deriving the closed-form expression for the phase noise in a chain of LC oscillators. Based on (4) and (11), the linearized phase noise model (19) is rewritten as

$$\begin{aligned}\dot{\tau}_k(t) = &\left\{ \Gamma_M V_M \omega_c \cos\big[\omega_0 (t + \bar{\alpha}_k + mt) + \pi/2\big] \right. \\ &\left. \times \sum_{j=1}^{N} g_{kj} V_M \cos\big[\omega_0 \big(t + \bar{\alpha}_j + mt\big) + \pi/2\big] \right\} \tau_k(t) \\ &+ \Gamma_M V_M \omega_c \cos[\omega_0 (t + \bar{\alpha}_k + mt)] \\ &\times \sum_{j=1}^{N} g_{kj} \cos\big[\omega_0 \big(t + \bar{\alpha}_j + mt\big) + \pi\big]\ \tau_j(t) + n_{\text{eq}}^k(t).\end{aligned} \tag{25}$$

Then, we exploit averaging again and keep only the low-frequency terms arising from the cosine products, obtaining

$$\begin{aligned}\dot{\tau}_k(t) \approx &B\left(\sum_{j=1}^{N} g_{kj}\cos\big(\bar{\phi}_k - \bar{\phi}_j\big)\right) \times \tau_k(t) \\ &- B\sum_{j=1}^{N} g_{kj}\cos\big(\bar{\phi}_k - \bar{\phi}_j\big) \times \tau_j(t) + n_{\text{eq}}^k(t).\end{aligned} \tag{26}$$

Multiplying both sides of (26) by ω_0 and noticing that the excess phase fluctuation is

$$\theta_k(t) = \omega_0 \tau_k(t). \tag{27}$$

Equation (26) can be rewritten in the following compact form:

$$\frac{d}{dt}\vec{\theta}(t) = \mathbf{A} \times \vec{\theta}(t) + \omega_0 \vec{n}_{\text{eq}}(t) \tag{28}$$

where $\vec{\theta}(t)$ and $\vec{n}_{\text{eq}}(t)$ are the vectors that collect the excess phase fluctuations variables and the equivalent noise sources of the oscillators, respectively. The elements of matrix $\mathbf{A} \in \mathbb{R}^{N\times N}$ are decided by

$$\begin{aligned}a_{kk} &= B \sum_{j=1, j\neq k}^{N} g_{kj}\cos\big(\bar{\phi}_k - \bar{\phi}_j\big) \\ a_{kj} &= -B\, g_{kj}\cos\big(\bar{\phi}_k - \bar{\phi}_j\big) \quad \text{for } k \neq j.\end{aligned} \tag{29}$$

It is worth noting that the matrix $\mathbf{A} = \mathbf{A}(\bar{\phi}_1, \bar{\phi}_2, \ldots, \bar{\phi}_N)$ is a function of the phase difference values which are established at synchronization regime. From (28) we see that the eigenvalues of such a matrix govern the dynamics induced by any perturbation of the synchronization phase values [18]. Thus a given phase set $\bar{\phi}_1, \bar{\phi}_2, \ldots, \bar{\phi}_N$ is stable if and only if the eigenvalues λ_k of $\mathbf{A}$ are such that: one eigenvalue is zero, i.e., $\lambda_1 = 0$, and the remaining ones have negative real part $\Re(\lambda_k) < 0$ for $k = 2, \ldots, N$. As a result, the computation of matrix $\mathbf{A}$ and of its eigenvalues provides a robust way to establish the stability of a given phase separation simulated with the phase-domain model (8).

Finally, to compute the array phase noise, the system (28) is transformed in the frequency domain and the Fourier transform

of $\vec{\theta}(t)$ is calculated to be

$$\vec{\theta}(f) = \mathbf{T}(f) \times \left(\omega_0 \vec{N}_{\rm eq}(f)\right) \tag{30}$$

where $\mathbf{T}(f) = \{t_{kj}(f)\}$ is the inverse matrix

$$\mathbf{T}(f) = (j2\pi f \mathbf{I}_N - \mathbf{A})^{-1} \tag{31}$$

$\mathbf{I}_N$ is the identity matrix of size N while "-1" denotes matrix inverse operator. Since the equivalent noise sources $n^k_{\rm eq}(t)$ of different oscillators are mutually independent, the phase noise of the kth oscillator in the array is given by

$$S_{\theta_k}(f) = \sum_{j=1}^{N} |t_{kj}(f)|^2 \, \omega_0^2 \, S_{n_j}(f). \tag{32}$$

Each entry $t_{kj}(f)$ in the matrix (31) has an intuitive interpretation: its squared module represents the noise transfer function from the noise sources in the jth oscillator toward the phase variable of the kth oscillator in the chain array.

V. Numerical Experiments

In this section, we study a multiphase chain array formed with N LC oscillators. The schematic of each LC oscillator is shown in Fig. 1 and the device parameters are listed in Table I. Transistor models are from a 0.28 μm CMOS technology. The oscillator is first simulated with the periodic steady state (pss) analysis of SpectreRF and then the $\Gamma(t)$ function is extracted with the method described in [21]. Fig. 2 in Section II reports the output voltage $V_0(t)$ measured across the LC tank and the $\Gamma(t)$ function (scaled by the factor 50). In the remainder, we present the results for a chain array with the topology and parameter settings shown in Fig. 7. The transconductance parameter is fixed $g = 10^{-5}\,\Omega^{-1}$ which corresponds to a weak coupling among oscillators. The sign plus or minus in Fig. 7 refers to the way a transconductance source is connected to the nodes of the injected oscillator, as shown in Fig. 5.

Fig. 8 reports the phase variables simulated with the phase-domain model (8) for setting 1) which corresponds to a bidirectional open chain. The initial phase values are selected randomly in the interval $(0, 2\pi)$. Asymptotically, for $t \to \infty$, all phase variables approach the same waveform, meaning that all oscillators synchronize in phase (i.e., output voltages are perfectly superimposed). We note also that the asymptotic waveform in Fig. 8 has a finite negative slope m which corresponds to a negligible reduction of the oscillating frequency ω_c (15) compared to the free-running one ω_0. A similar result (not shown for brevity) is obtained for setting 2) which corresponds to a closed unidirectional chain with feedback.

For setting 5), shown in Fig. 9, instead we obtain that the phase variables of two consecutive oscillators are such that $\phi_{k+1}(t) - \phi_k(t) = \pm\pi$. This means that the output voltages of different oscillators are in phase or in antiphase. We conclude that settings 1), 2), and 5) are not useful for applications (for a chain array of identical devices), since they do not allow achieving fine phase separation even if we increase the number N of stages.

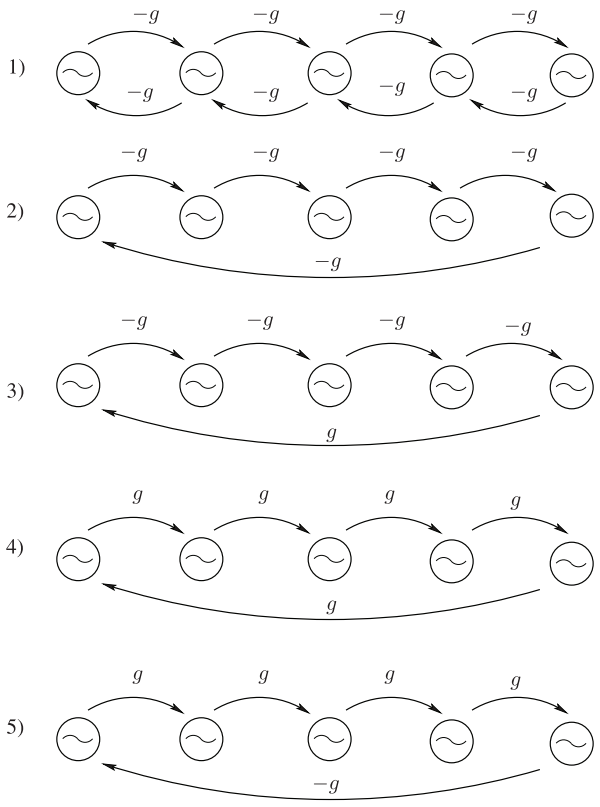

Fig. 7. Chain array with five different topology and parameter settings.

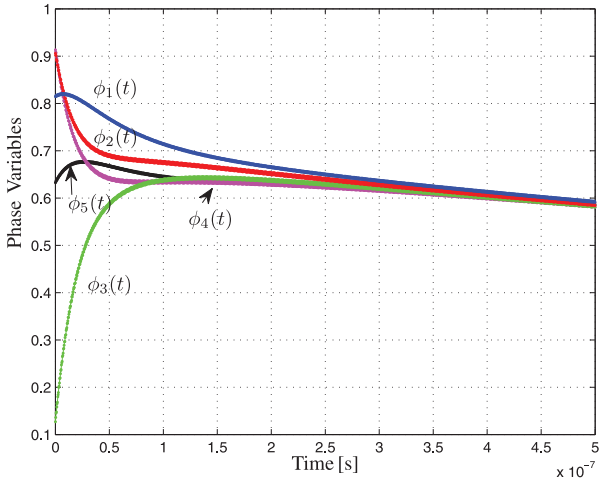

Fig. 8. Setting 1): phase variables converge to the same waveform.

The first case relevant for applications is that of setting 3) where the phase variables shown in Fig. 10 are such that $\phi_{k+1}(t) - \phi_k(t) = -\pi/N$. Repeated phase-domain simulations reveal that for setting 3) a regular phase separation is established in the chain array and that such separation can be made finer by increasing the number N of oscillators. In addition, all the eigenvalues (but the first which is zero) of the matrix $\mathbf{A}$ in (28) have negative real part confirming the stability of such phase configurations. Fig. 11 reports the output voltages $V_k(t)$ of the oscillator array for setting 3) obtained after substituting the simulated phase waveforms into the phase-domain model (2).

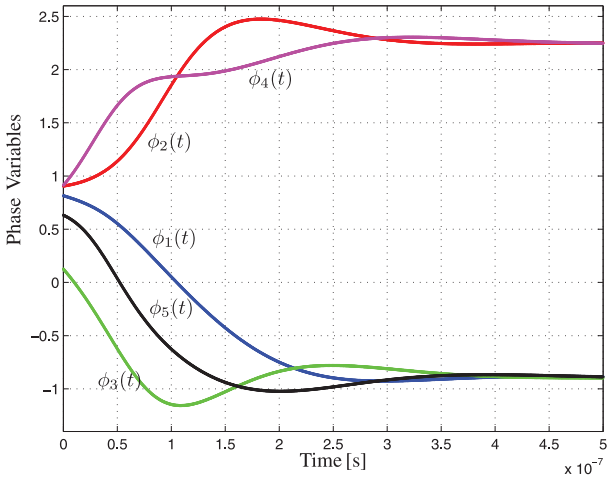

Fig. 9. Setting 5): phase variables divide into two clusters.

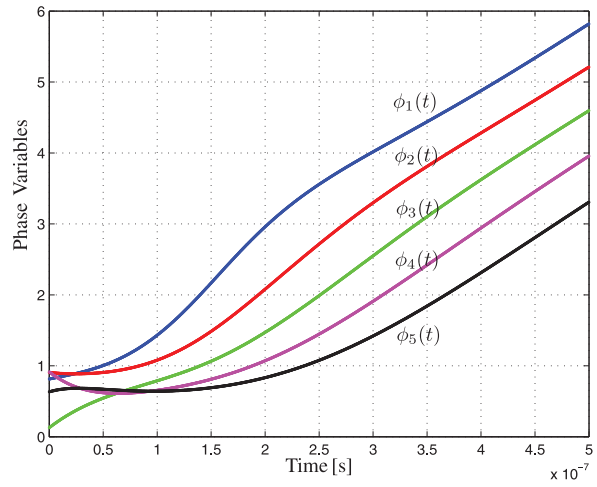

Fig. 10. Setting 3): phases are separated by $-\pi/N$.

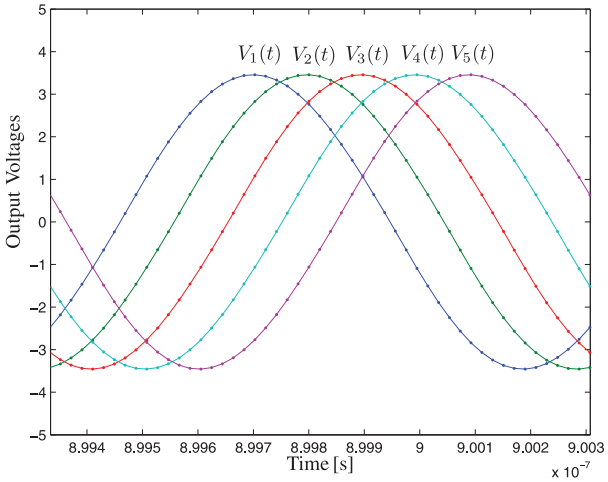

Fig. 11. Output voltages simulated with the phase-domain model for setting 3).

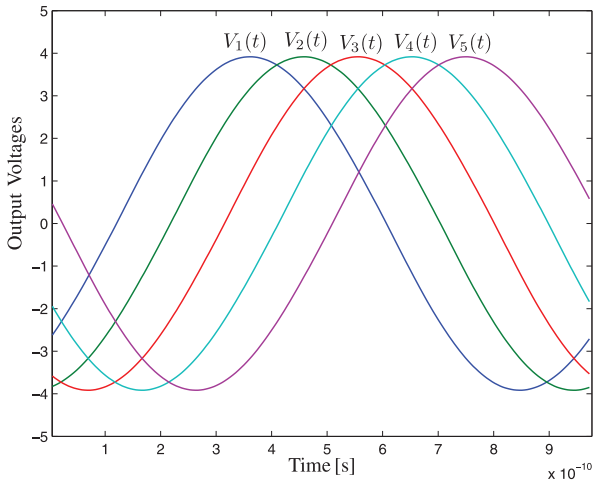

Fig. 12. Output voltages simulated with Spectre for setting 3).

To verify the correctness of our phase-domain predictions for setting 3), detailed circuit-level simulations of the chain array are performed with SpectreRF. The array output voltages yielded by SpectreRF are plotted in Fig. 12 and fully confirm the predicted phase separations as well as the validity of weak coupling hypothesis for the selected transconductance parameter value g. It is worth noting here that the circuit-level simulation of a weakly coupled oscillator array can be very tricky and/or time-consuming. If oscillators are all identical (and weakly coupled), the array admits a trivial periodic steady solution (pss) with the output voltages of all oscillators perfectly superimposed. For setting 3), this perfectly in-phase solution is unstable and thus it is a spurious solution. To avoid that the pss analysis of SpectreRF converges to this spurious solution, long transient initializations (starting from nonidentical initial conditions) and tight tolerance have to be imposed which results in long simulation time. For these reasons, circuit-level simulations are not suitable to explore the numerous phase separation cases that can occur in a large chain array but they may be used for cross validations in a few cases.

Another case which is relevant for applications is setting 4): the phase variables shown in Fig. 13 are such that $\phi_{k+2}(t) - \phi_k(t) = 2\pi/N$. In this case, a regular phase separation is established between the kth and the $(k+2)$th oscillator in the chain. Repeated phase simulations reveal that such phase separation is actually obtained only when N is odd while for an even number of oscillators phases divide in two clusters like in Fig. 9. We conclude that settings 3) and 4) (with N odd) achieves the desired phase separation. We also verified that the same result holds when parameter settings 3) and 4) are implemented in a bidirectional symmetric chain array. The realization of bidirectional coupling (i.e., where each oscillator is connected to the next and previous oscillators) costs more in terms of number of devices (and thus of area occupation), however, the theoretical results presented in [5] suggest that symmetric arrays may give better phase noise performance than unsymmetric ones. In what follows we investigate this issue for the case of setting 3).

First, with the phase noise analysis of SpectreRF, we simulate the phase noise spectrum of one free-running LC oscillator. Above some kilohertz, this spectrum is dominated

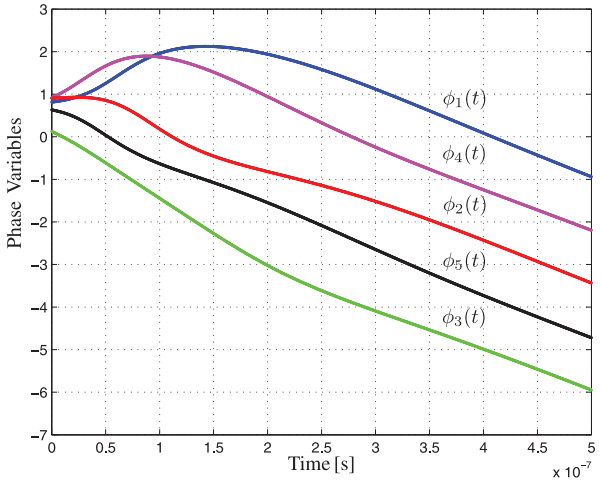

Fig. 13. Setting 4): phases are such that $\phi_{k+2}(t) - \phi_k(t) = -2\pi/N$.

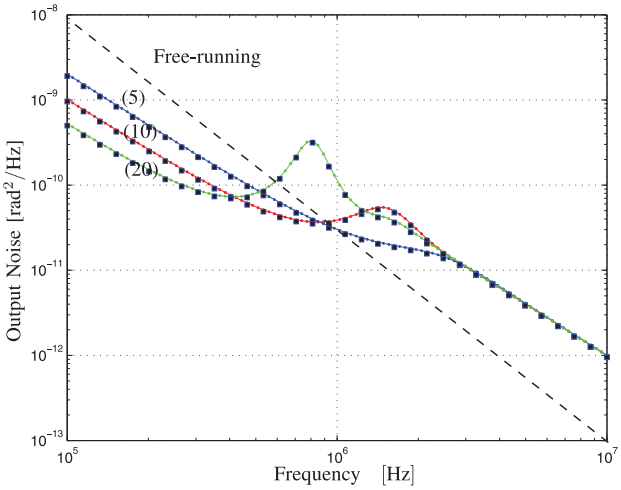

Fig. 14. Phase noise for setting 3) in a unidirectional array formed of $N = 5, 10, 20$ stages. (Continuous lines) closed-form expression (32). (Filled square markers) *pnoise* of SpectreRF.

by the white noise internal sources and corresponds to the noise parameter $S_{\text{eq}}^{W} = 10^{-16}\,\text{rad}^2/\text{Hz}$ in (6). This parameter corresponds to a noise level $S_\phi(f)$ of about $10^{-10}\,\text{rad}^2/\text{Hz}$ at frequency offset $f = 1\,\text{MHz}$.

Second, with the closed-form expression (32) we compute the phase noise spectrum $S_{\theta_k}(f)$ of one oscillator in a chain array composed of N stages. For the case of unidirectional coupling, this phase noise is plotted in Fig. 14 for increasing values of chain stages N. We see how the array phase noise is reduced compared to that of the free-running oscillator (shown in Fig. 14 with a dashed line) at frequencies lower than 500 kHz and how such a reduction gets more effective for higher values of N. However, we also see that increasing N results in a phase noise deterioration with the appearance of a spur around 1 MHz. The phase noise in the bidirectional array, shown in Fig. 15, instead exhibits a uniform reduction of the noise spectrum over a much wider frequency range and without deteriorating spurs. A symmetric bidirectional coupling is thus recommended in all those applications where the above mentioned noise spurs are not tolerable. The above reported results have been fully confirmed by the simulation results

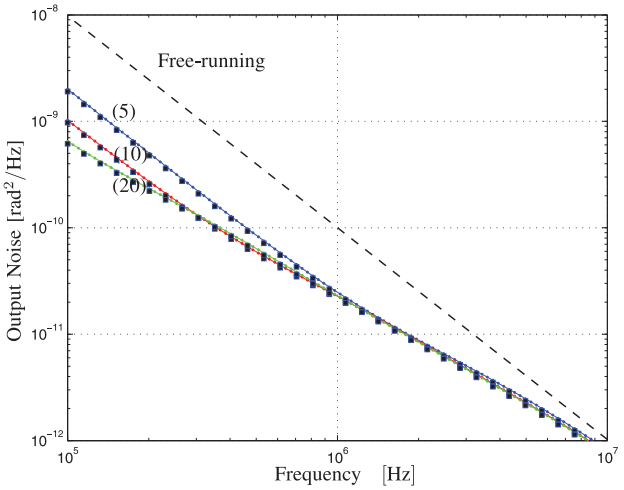

Fig. 15. Phase noise for setting 3) in a symmetric bidirectional array $N = 5, 10, 20$ stages. (Continuous lines) closed-form expression (32). (Filled square markers) *pnoise* of SpectreRF.

from SpectreRF plotted in Figs. 14 and 15 with filled squared markers. The phase noise analysis *(pnoise)* with SpecteRF of the unidirectional array formed with $N = 20$ oscillators takes about forty minutes on a quad-core workstation. By comparison, the phase-domain simulation of (8) and noise calculation with (32) is accomplished in a few seconds, i.e., it is about three orders of magnitude faster.

VI. Conclusion

In this paper, we have described a phase-domain modeling technique to simulate in a very efficient way an array of weakly coupled oscillators. The method allows determining the stable phase separations that are established at synchronization as a function of array topology and parameter settings. For the relevant case of a chain array of LC oscillators, we have identified two topologies that achieve the desired phase separation in a stable way. Finally, an original closed-form expression for the chain array phase noise has been derived and its accuracy has been verified against detailed SpectreRF simulations. Phase-domain simulations reveal that the phase noise of an oscillator in the array is reduced compared to that of the same oscillator working in free-running. Noise reduction becomes more effective when the number of stages is increased and oscillators are coupled in a bidirectional way.

References

[1] R. van de Beek, E. Klumperink, C. Vaucher, and B. Nauta, "Low-jitter clock multiplication: A comparison between PLLs and DLLs," *IEEE Trans. Circuits Syst. II, Analog Digit. Signal Process.*, vol. 49, no. 8, pp. 555–566, Aug. 2002.

[2] K. Lee *et al.*, "A single-chip 2.4-GHz direct-conversion CMOS receiver for wireless local loop using multiphase reduced frequency conversion technique," *IEEE J. Solid-State Circuits*, vol. 36, no. 5, pp. 800–809, May 2001.

[3] R. Marathe *et al.*, "Resonant body transistors in IBMs 32 nm SOI CMOS technology," *J. Microelectromech. Syst.*, vol. 23, no. 3, pp. 636–650, Jun. 2014.

[4] L. Romanò, S. Levantino, C. Samori, and A. L. Lacaita, "Multiphase LC oscillators," *IEEE Trans. Circuits Syst. I, Reg. Papers*, vol. 53, no. 7, pp. 1579–1588, Jul. 2006.

[5] H. C. Chang, X. Cao, U. K. Mishra, and R. York, "Phase noise in coupled oscillators: Theory and experiment," *IEEE Trans. Microw. Theory Techn.*, vol. 45, no. 5, pp. 605–615, May 1997.
[6] G. B. Ermentrout and N. Kopell, "Frequency plateaus in a chain of weakly coupled oscillators," *SIAM J. Math. Anal.*, vol. 15, no. 2, pp. 215–237, 1984.
[7] D. Harutyunyan, J. Rommes, J. ter Maten, and W. Schilders, "Simulation of mutually coupled oscillators using nonlinear phase macromodels applications," *IEEE Trans. Comput.-Aided Design Integr. Circuits Syst.*, vol. 28, no. 10, pp. 1456–1466, Oct. 2009.
[8] D. Harutyunyan and J. Rommes, "Simulation of coupled oscillators using nonlinear phase macromodels and model order reduction," in *Model Reduction for Circuit Simulation* (Lecture Notes in Electrical Engineering), vol. 74, P. Benner, M. Hinze, and E. J. W. ter Maten, Eds. Dordrecht, The Netherlands: Springer, 2011, pp. 163–176.
[9] P. Maffezzoni, "Synchronization analysis of two weakly coupled oscillators through a PPV macromodel," *IEEE Trans. Circuits Syst. I, Reg. Papers*, vol. 57, no. 3, pp. 654–663, Mar. 2010.
[10] F. X. Kaertner, "Analysis of white and $f^{-\alpha}$ noise in oscillators," *Int. J. Circuit Theory Appl.*, vol. 18, no. 5, pp. 485–519, 1990.
[11] A. Demir, A. Mehrotra, and J. Roychowdhury, "Phase noise in oscillators: A unifying theory and numerical methods for characterisation," *IEEE Trans. Circuits Syst. I, Fundam. Theory Appl.*, vol. 47, no. 5, pp. 655–674, May 2000.
[12] A. Demir, "Computing timing jitter from phase noise spectra for oscillators and phase-locked loops with white and $1/f$ noise," *IEEE Trans. Circuits Syst. I, Reg. Papers*, vol. 53, no. 9, pp. 1859–1874, Sep. 2006.
[13] P. Vanassche, G. Gielen, and W. Sansen, "On the difference between two widely publicized methods for analyzing oscillator phase behavior," in *Proc. IEEE/ACM Int. Conf. Comput.-Aided Design (ICCAD)*, San Jose, CA, USA, Nov. 2002, pp. 229–233.
[14] M. I. Freidlin and A. D. Wentzell, *Random Perturbations of Dynamical Systems*. Berlin, Germany: Springer, 1984.
[15] A. Rofougaran *et al.*, "A single-chip 900-MHz spread-spectrum wireless transceiver in 1-μm CMOS. I. architecture and transmitter design," *IEEE J. Solid-State Circuits*, vol. 33, no. 4, pp. 515–534, Apr. 1998.
[16] P. Maffezzoni and S. Levantino, "Analysis of VCO phase noise in charge-pump phase-locked loops," *IEEE Trans. Circuits Syst. I, Reg. Papers*, vol. 59, no. 10, pp. 2165–2175, Oct. 2012.
[17] A. Pikovsky, M. Rosenblum, and J. Kurths, *Synchronization*. Cambridge, U.K.: Cambridge Univ. Press, 2001.
[18] M. Farkas, *Periodic Motions*. New York, NY, USA: Springer, 1994.
[19] M. M. Gourary, S. G. Rusakov, S. L. Ulyanov, M. M. Zharov, and B. J. Mulvaney, "Evaluation of oscillator phase transfer functions," in *Scientific Computing in Electrical Engineering SCEE 2008* (Mathematics in Industry), vol. 14, J. Roos and L. R. J. Costa, Eds. Berlin, Germany: Springer, 2010.
[20] *Virtuoso Spectre Circuir Simulator RF Analysis User Guide*, Product Version 7.2, Cadence Design Syst., San Jose, CA, USA, May 2010.
[21] S. Levantino and P. Maffezzoni, "Computing the perturbation-projection-vector of oscillators via frequency domain analysis," *IEEE Trans. Comput.-Aided Design Integr. Circuits Syst.*, vol. 31, no. 10, pp. 1499–1507, Oct. 2012.

Paolo Maffezzoni (M'08) received the Laurea degree *(summa cum laude)* in electrical engineering from the Politecnico di Milano, Milan, Italy, and the Ph.D. degree in electronic instrumentation from the Università di Brescia, Brescia, Italy, in 1991 and 1996, respectively.

In 1998, he became an Assistant Professor, and subsequently, an Associate Professor of Electrical Engineering with the Politecnico di Milano. His current research interests include analysis and simulation of nonlinear circuits and systems, oscillating devices modeling, synchronization, and stochastic simulation. He has over 120 research publications, among which 60 papers were published in international journals.

Prof. Maffezzoni is currently serving as an Associate Editor of the IEEE TRANSACTIONS ON COMPUTER-AIDED DESIGN OF INTEGRATED CIRCUITS AND SYSTEMS.

Bichoy Bahr (S'10) received the B.Sc. (Hons.) and M.Sc. degrees, both in electrical engineering, from Ain Shams University, Cairo, Egypt, in 2008 and 2012, respectively. He is currently pursuing the Ph.D. degree in electrical engineering from the Massachusetts Institute of Technology (MIT), Cambridge, MA, USA.

He served as an Analog/Mixed Signal and Microelectromechanical Systems (MEMS) Modeling/Design Engineer with MEMS Vision, Cairo. He is currently a Research Assistant with HybridMEMS Group, MIT. His current research interests include the design, fabrication, modeling and optimization of monolithically integrated unreleased MEMS resonators, in standard integrated circuits technology, multiGHz MEMS-based monolithic oscillators, coupled oscillator-arrays, and unconventional signal processing.

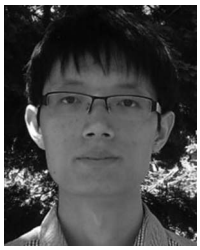

Zheng Zhang (S'09) received the B.Eng. degree from the Huazhong University of Science and Technology, Wuhan, China, and the M.Phil. degree from the University of Hong Kong, Hong Kong, in 2008 and 2010, respectively. He is currently pursuing the Ph.D degree in electrical engineering and computer science from the Massachusetts Institute of Technology (MIT), Cambridge, MA, USA.

Since 2011, he has been collaborating with Coventor Inc., Cary, NC, USA, on numerical methods for microelectromechanical systems (MEMS) simulation. His current research interests include uncertainty quantification and tensor analysis, with applications in integrated circuits, MEMS, power systems, silicon photonics, and other emerging engineering problems.

Mr. Zhang was the recipient of the 2014 IEEE TRANSACTIONS ON COMPUTER-AIDED DESIGN OF INTEGRATED CIRCUITS AND SYSTEMS Best Paper Award, the 2011 Li Ka Shing Prize (University Best M.Phil./Ph.D. Thesis Award) from the University of Hong Kong, Hong Kong, and the 2010 Mathworks Fellowship from the MIT.

Luca Daniel (S'98–M'03) received the Ph.D. degree in electrical engineering and computer science from the University of California, Berkeley (UC Berkeley), Berkeley, CA, USA, in 2003.

He is currently an Associate Professor with the Department of Electrical Engineering and Computer Science, Massachusetts Institute of Technology (MIT), Cambridge, MA, USA. His current research interests include development of integral equation solvers for very large complex systems, uncertainty quantification and stochastic solvers for large number of uncertainties, and automatic generation of parameterized stable compact models for linear and nonlinear dynamical systems, simulation, modeling, and optimization for mixed-signal/RF/mm-wave circuits, power electronics, microelectromechanical systems, nanotechnologies, materials, magnetic resonance imaging scanners, and the human cardiovascular system.

Prof. Daniel was the recipient of the 1999 IEEE TRANSACTIONS ON POWER ELECTRONICS Best Paper Award, the 2003 Best Ph.D. Thesis Awards from both the Electrical Engineering and the Applied Math Departments, UC Berkeley, the 2003 ACM Outstanding Ph.D. Dissertation Award in Electronic Design Automation, five Best Paper Awards in international conferences, and nine additional nominations, the 2009 IBM Corporation Faculty Award, the 2010 IEEE Early Career Award in Electronic Design Automation, and the 2014 IEEE TRANSACTIONS ON COMPUTER-AIDED DESIGN Best Paper Award.